




Cite this: *Chem. Commun.*, 2024, 60, 14057

Received 21st September 2024,  
Accepted 6th November 2024

DOI: 10.1039/d4cc04899g

rsc.li/chemcomm

# Visible light-activated polyphenol–Al<sup>3+</sup> coordination for ambient and quantitative xylose-to-furfural conversion†

Jinshu Huang, Qizhi Luo, Tengyu Liu, Song Yang and Hu Li \*

**Bio-based xylose-to-furfural conversion is often accompanied by condensation/degradation at evaluated thermal conditions. This study presents a combined strategy of visible light-enhanced acidity and local photothermal effect for room-temperature cascade isomerization-dehydration of xylose to furfural in an ultrahigh yield (96.3%), in which Lewis acidic Al<sup>3+</sup> centers facilitate electron transfer from xylose to initiate isomerization and the formation of Al<sup>3+</sup>-polyphenol complex is enabled to release Brønsted acid for dehydration while co-added bio-graphene *in situ* offers satisfactory photothermal conditions.**

Developing renewable energy and declining dependence on fossil fuels are of great significance for achieving the goal of carbon neutrality.<sup>1</sup> Biomass is an inexhaustible carbon resource for clean energy, which can be upgraded to biofuels and versatile platform chemicals (e.g., formic acid, methanol, ethanol, lactic acid, levulinic acid, 5-hydroxymethylfurfural, and furfural).<sup>2</sup> In particular, furfural is a strategically important compound for the widespread synthesis of functional molecules (e.g., valerate, furfuryl alcohol, 5-methyltetrahydrofuran, and 2-furancarboxylic acid) applied in fuel additives, plastics, organic solvents, pharmaceuticals, and agrochemicals, which has been recognized by the U.S. Department of Energy as one of the 14 most promising and important chemicals.<sup>3</sup>

In 2022, the global output of furfural was 700 000 tons, with a market size of USD 556.7 million. It is expected to continue to rise at a growth rate of 7.0% from 2024 to 2030.<sup>4</sup> At present, furfural is mainly derived from the direct conversion of xylose, or isomerization of xylose to xylulose followed by dehydration. In general, xylose can be directly transformed into furfural over homogeneous Brønsted acid (e.g., HCl and H<sub>2</sub>SO<sub>4</sub>) at a high temperature (>180 °C), but side reactions like condensation

(humins) and degradation (e.g., formic acid, acetic acid, and pyruvic acid) occur during this process, which results in a low yield of furfural (40–50%), carbon loss, acidic wastewater generation, and equipment corrosion.<sup>5</sup> Given this, many solid SO<sub>3</sub>H-functionalized catalysts (e.g., Nafion and MCM-41-SO<sub>3</sub>H) have been reported,<sup>6,7</sup> which are recyclable and afford low to moderate yields of furfural (27–75%), due to the lack of Lewis acid sites that can catalyze the initial isomerization of xylose to xylulose. Also, a relatively long reaction time (2–24 h), and high energy consumption/temperature (140–170 °C) are usually required. On the other hand, various Lewis acidic metal halide/oxide catalysts (e.g., SnCl<sub>4</sub>, CrCl<sub>3</sub>, and ZnO)<sup>8</sup> are developed but lack Brønsted acid sites, which is not conducive to the second-step dehydration of xylulose to furfural, also leading to unsatisfactory furfural yields (9.8–63%) and harsh reaction conditions. As a promising alternative, bifunctional catalysts consisting of Lewis and Brønsted acid sites (CrCl<sub>3</sub>/HCl, Sn-beta/HCl, and zeolites) are exploited,<sup>2b,4,5,9</sup> showing superior performance for xylose-to-furfural conversion (up to 90% yield) compared to the above single-site catalysts (typically <80% yields). The selectivity/yield of furfural is dependent on appropriately regulating the distribution of Lewis and Brønsted acid sites responsible for the xylose-to-xylulose isomerization and xylulose-to-furfural dehydration, respectively. In addition, biphasic systems (e.g., toluene/H<sub>2</sub>O and THF/H<sub>2</sub>O) are emerging to avoid side reactions, to some extent.<sup>9</sup> However, a long-term and high-temperature driving process cannot be avoided in these thermocatalytic systems.

Here, this study presents a visible-light-enhancing protocol for coordination of Al<sup>3+</sup> and fulvic acid (FA) to regulate *in situ* generation of Lewis/Brønsted acid sites, which can drive the cascade isomerization-dehydration of xylose to furfural of high efficiency. The coordinated complex (FA + Al<sup>3+</sup>) shows obvious absorption of visible light, which not only promotes the electron transfer from xylose to the Al<sup>3+</sup> center (*i.e.*, ligand-to-metal charge transfer (LMCT) effect), capable of reducing the electron density of the β-C–H bond in xylose to initiate isomerization, but also facilitates the coordination of FA and Al<sup>3+</sup> to release Brønsted acid for the succeeding dehydration. Meanwhile,

State Key Laboratory of Green Pesticide, Key Laboratory of Green Pesticide & Agricultural Bioengineering, Ministry of Education, State-Local Joint Laboratory for Comprehensive Utilization of Biomass, Center for R&D of Fine Chemicals, Guizhou University, Guiyang, Guizhou 550025, China. E-mail: hli13@gzu.edu.cn

† Electronic supplementary information (ESI) available. See DOI: <https://doi.org/10.1039/d4cc04899g>

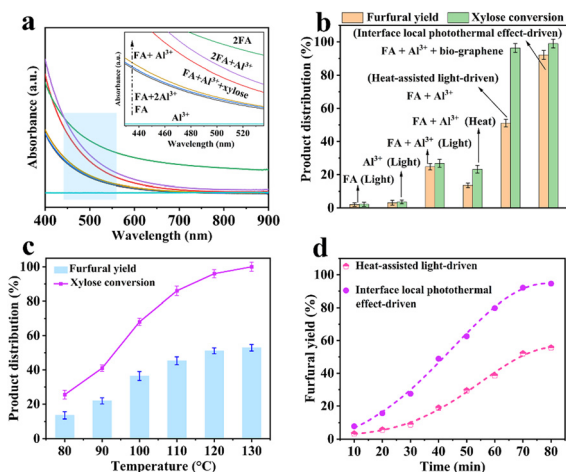


**Fig. 1** (a) The UV-vis absorption spectra of 0.01 M  $\text{Al}^{3+}$ , 0.1 M xylose, and 9 g  $\text{L}^{-1}$  FA in 2 mL DMSO. (b) Different catalytic systems for conversion of xylose to furfural (conditions: 0.01 M  $\text{Al}^{3+}$ , 0.1 M xylose, and 9 g  $\text{L}^{-1}$  FA in 2 mL DMSO at 1500  $\text{W m}^{-2}$  light intensity or 120 °C for 70 min). (c) Effect of reaction temperature on furfural yield (conditions: 0.01 M  $\text{Al}^{3+}$ , 0.1 M xylose, and 9 g  $\text{L}^{-1}$  FA in 2 mL DMSO for 70 min). (d) Reaction kinetics with different catalytic systems.

under visible-light irradiation, the interfacial local photothermal effect resulting from bio-graphene in the reaction system can further boost the LMCT and release of Brønsted acid, effectively avoiding side reactions caused by traditional high-temperature heating of bulk solution, thus furnishing furfural in an ultrahigh yield (up to 96.3%) at room temperature. This is an innovative visible-light-stimulating strategy of enhancing the LMCT effect and releasing Brønsted acidity for energy-saving/green multi-step catalytic conversion of biomass feedstock.

As the largest reserve of metallic element in the earth's crust, aluminum (Al) has limited light absorption (almost no light absorption)<sup>10</sup> which does not change with varying concentrations of  $\text{Al}^{3+}$  (Fig. 1a). Due to its weak photoredox ability, the direct use of  $\text{Al}^{3+}$  is typically unfavorable for the photocatalytic reaction. Surprisingly, when 9 g  $\text{L}^{-1}$  FA ligand was added to 0.01 M  $\text{Al}^{3+}$  DMSO solution, the obtained  $(\text{FA} + \text{Al}^{3+})$  complex was found to have good light absorption properties in the visible region. Upon the addition of xylose (0.1 M;  $\text{FA} + \text{Al}^{3+} + \text{xylose}$ ), the absorption was further enhanced, suggesting the electron transfer from xylose to the  $(\text{FA} + \text{Al}^{3+})$  complex (*i.e.*, LMCT). As the FA concentration was 18 g  $\text{L}^{-1}$  in 0.01 M  $\text{Al}^{3+}$  solution, the light absorption range of relevant  $(2\text{FA} + \text{Al}^{3+})$  complex increased significantly, indicating that increasing the FA concentration can expand the light absorption range of the corresponding complexes, associated with increased  $\text{H}^+$  release capability and potentially improved photocatalytic performance. On the contrary, the light absorption range of the complexes did not increase significantly when  $\text{Al}^{3+}$  was excessively increased in  $(\text{FA} + 2\text{Al}^{3+})$  solution, further clarifying that the absorption of  $\text{Al}^{3+}$  to light was limited. The catalytic systems of keeping xylose feed (0.1 M) unchanged, the complex of  $(\text{FA} + \text{Al}^{3+})$ , FA, and  $\text{Al}^{3+}$  were used to promote xylose conversion under visible-light irradiation (1500  $\text{W m}^{-2}$ ), affording furfural in yield of 24.8%, 2.1%, and 3.4%, respectively

(Fig. 1b). The results further illustrate that the presence of FA can assist  $\text{Al}^{3+}$  to significantly improve the overall photocatalytic activity.

Both light and heat can be employed as energy sources for producing furfural from xylose. At xylose,  $\text{Al}^{3+}$ , and FA ligand concentrations of 0.1 M, 0.01 M, and 9 g  $\text{L}^{-1}$ , respectively, the effects of light-, heat-, heat-assisted light-, and interface local photothermal effect-driven systems on the xylose-to-furfural conversion were investigated (Fig. 1b). Under visible-light irradiation, negligible furfural yields (2.1–3.4%) were observed at xylose conversion of 2.3–3.7% in the presence of  $\text{Al}^{3+}$  or FA. The complex of  $(\text{FA} + \text{Al}^{3+})$  could afford a relatively higher furfural yield (13.6%) with increased xylose conversion (23.2%) at 120 °C (Fig. 1b), indicating that the heat-driven catalytic system of  $(\text{FA} + \text{Al}^{3+})$  has sufficient Lewis acid sites for isomerization of xylose to xylulose while cannot be induced to coordinate and produce Brønsted acid sites for xylulose dehydration. In contrast, both xylose conversion (26.8%) and furfural yield (24.8%) could be further enhanced at visible-light illumination (Fig. 1b), showing that the light-induced coordination of  $\text{Al}^{3+}$  and FA can provide Brønsted acid for the dehydration of xylulose. Moreover, the light-driven LMCT effect between  $\text{Al}^{3+}$  and xylose can promote the isomerization of xylose to xylulose but insufficiently, which is in line with the still dissatisfactory xylose conversion, possibly due to the inferior energy supply.

Interestingly, in the heat-assisted (120 °C) light-driven catalytic system, the yield of furfural significantly increased to 51.1% at an evaluated xylose conversion of 96.3% (Fig. 1b). In detail, furfural remained in a low yield (12.3–21.9%) at 80–90 °C (Fig. 1c), due to the inadequate force provided by heating to drive the  $\text{Al}^{3+}$  site to complete the xylose isomerization reaction. At a relatively high temperature of 100–130 °C, it is sufficient to activate the  $\text{Al}^{3+}$  coordination center for the xylose-to-xylulose isomerization enabled by the LMCT effect, and to release the Brønsted acid from the visible light-induced  $(\text{FA} + \text{Al}^{3+})$  coordination complex for the dehydration of xylulose to furfural (36.4–52.8%). At 120–130 °C, xylose was almost completely converted, but the yield of furfural remained about 52% (Fig. 1c), which is mainly attributed to the xylose condensation and furfural degradation under continuous high-temperature heating conditions.

After further adding graphene derived from *Chlorella* into the above reaction system  $(\text{FA} + \text{Al}^{3+} + \text{xylose})$ , light can induce photothermal effect, achieving xylose conversion rate > 99%, and furfural selectivity > 93% in the absence of exogenous heating (Fig. 1b). It can be concluded that the generated interfacial local photothermal effect can not only provide enough energy to drive the coordinated  $\text{Al}^{3+}$  center to complete the LMCT-enhanced isomerization of xylose, but also propel the formation of Brønsted acid for the subsequent xylulose dehydration, which is also evidenced by more evident impact of FA content on the light-irradiated process (Fig. S1, ESI†). Notably, the photothermal system avoids the continuous heating of bulk reaction solution at high temperatures, thus effectively circumventing side reactions like xylose condensation and furfural degradation.

To expound the role of bio-graphene in xylose-to-furfural conversion, Fig. 1d shows the kinetics of the reaction conducted at both the heat-assisted light irradiation (120 °C +

1500 W m<sup>-2</sup>, without adding graphene) and interfacial local photothermal condition (1500 W m<sup>-2</sup>, with graphene) after different times. It was found that the yield of furfural increased with the extension of reaction time in both systems under visible light irradiation, showing that light irradiation plays a role in promoting furfural production. In particular, the yield of furfural in the two reaction systems increased significantly after 40 min, indicating that the light enhances the formation of the (FA + Al<sup>3+</sup>) complex to release Brønsted acid after a relatively long period. Accordingly, the furfural yield of the catalytic system driven by the local photothermal effect at the interface is significantly higher than that of the thermally assisted photo-driven catalytic system. To further confirm the photo-induced coordination of Al<sup>3+</sup> and FA able to generate Brønsted acid, the liquid solutions in different FA amounts before and after illumination were examined by UV-vis (Fig. 2a and b). All the solutions exhibited significantly increased light absorption after illumination, confirming the generation of coordinated (xylose + FA + Al<sup>3+</sup>) complexes along with the release of H<sup>+</sup> from the hydroxyl groups in FA upon coordination with Al<sup>3+</sup>. Note that the light absorption of the solution at 11 g L<sup>-1</sup> FA after illumination is relatively weaker than that of 9 g L<sup>-1</sup> (Fig. 2b), attributed to the high concentration of FA that hinders the coordination of xylose with Al<sup>3+</sup>.

FA is mainly an aromatic mixture, which is derived from plants and low-rank coal.<sup>11</sup> To better understand the real active component, Fig. 2c shows the catalytic efficiency of different aromatic ligands in FA with Al<sup>3+</sup> for furfural synthesis from xylose in DMSO. The results suggested that Al<sup>3+</sup> with catechol or pyrogallol as the ligand exhibited superior performance, with furfural yield of 83.5% and 88.2%, respectively. It is illustrated that the main active ligands in FA are polyphenols. In the absence of light, poor to low yields of furfural (0–18.7%) were obtained, further

proving the significant effect of light on the furfural synthesis. The optimal concentrations of catechol and pyrogallol were found to be 7 and 5 g L<sup>-1</sup> under light irradiation, with furfural yields of 96.3% and 95.6%, respectively (Fig. S2 and S3, ESI†). Inferior furfural yields were obtained with other Lewis acidic metal ions due to photocatalytic redox reactions (Fig. S4, ESI†). Fig. S5a (ESI†) reveals the activity comparison between the state-of-the-art catalysts at high temperatures (up to 200 °C) and the polyphenol-Al<sup>3+</sup> complexes at visible-light irradiation in this study (25 °C) for the synthesis of furfural from xylose.<sup>2a,5–9,12</sup> It can be seen that the polyphenol-Al<sup>3+</sup> coordination catalysts achieve the goal of superior activity and energy saving endowed by the local photothermal effect, capable of avoiding side reactions caused by high-temperature heating processes.

For the coordination mode of polyphenol-Al<sup>3+</sup> complex, it is preliminarily speculated that the light irradiation may induce hydroxyl groups in polyphenol to coordinate with Al<sup>3+</sup> in a bidentate chelating mode to liberate H<sup>+</sup>, including both binuclear and mononuclear coordination centers (Fig. S5b, ESI†). Moreover, xylose is also coordinated with Al<sup>3+</sup> through a similar bidentate chelating mode after replacing the weak ligand (H<sub>2</sub>O and DMSO) on the coordination catalyst. The addition of excessive polyphenol ligands will occupy the position of weak ligands, which makes it difficult for xylose to coordinate with Al<sup>3+</sup>, thus hindering the conversion of xylose. Therefore, the appropriate concentration of polyphenol ligands is the key to the efficient synthesis of furfural from xylose. Importantly, the hydroxyl groups in polyphenols would release protons after light-induced coordination with Al<sup>3+</sup>, offering sufficient Brønsted acid sites for the dehydration of the isomerization product xylulose to produce furfural (Fig. S6, ESI†). The above process needs light irradiation to occur, indicating that the xylose conversion and Brønsted acid generation are carried out in the excited state of the Al<sup>3+</sup> complex, which is thus elucidated by photoluminescence emission spectra. As shown in Fig. S5c (ESI†), the emission spectra (λ<sub>em</sub>) of the reaction solution change with the excitation spectra (λ<sub>ex</sub>), and a relatively short excitation wavelength benefits the enhanced emission spectrum intensity. Also, the furfural yield decreases (76.8% to 3.2%) with the increase of excitation wavelength from 400 to 640 nm (Fig. S5d, ESI†), conformably demonstrating that a shorter wavelength (*i.e.*, higher energy) is more conducive to the synthesis of furfural from xylose. More specifically, the complex of xylose and polyphenol-Al<sup>3+</sup> is transformed into an excited electronic state after absorbing light (>625nm), closely correlated with the LMCT effect,<sup>13</sup> which can transfer the electron of xylose to the Al<sup>3+</sup> coordination center, thereby reducing the electron density of the β-C-H bond in xylose to accelerate isomerization.<sup>27</sup> Al NMR spectrum of Al(NO<sub>3</sub>)<sub>3</sub>·9H<sub>2</sub>O in DMSO-d<sub>6</sub> disclosed that Al<sup>3+</sup> is in octahedral coordination structure (Fig. 3a), which is related to [Al(H<sub>2</sub>O)<sub>6</sub>]<sup>3+</sup> and [Al(OH)(H<sub>2</sub>O)<sub>5</sub>]<sup>2+</sup> species.<sup>13</sup> After catechol (a model ligand) was added to the above solution, two weak signal peaks at 1.9 and 1.6 ppm were detected in <sup>27</sup>Al NMR, indicating the catechol-Al<sup>3+</sup> complex formation. Further addition of xylose to the above (Al<sup>3+</sup> + catechol) complex solution did not appear additional signal without affecting original peaks, illustrating the instantaneous coordination of xylose molecules with

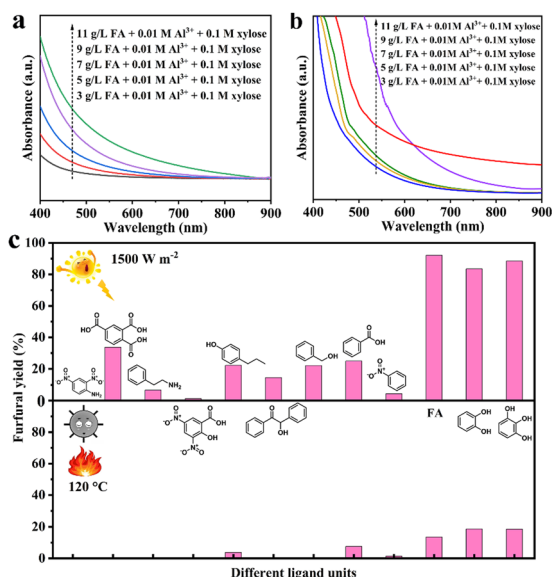


Fig. 2 (a) and (b) UV-Vis spectra of the reaction system at different FA dosages before and after illumination. (c) Catalytic conversion of xylose to furfural with Al<sup>3+</sup> and different ligands under thermal and light-irradiation conditions.

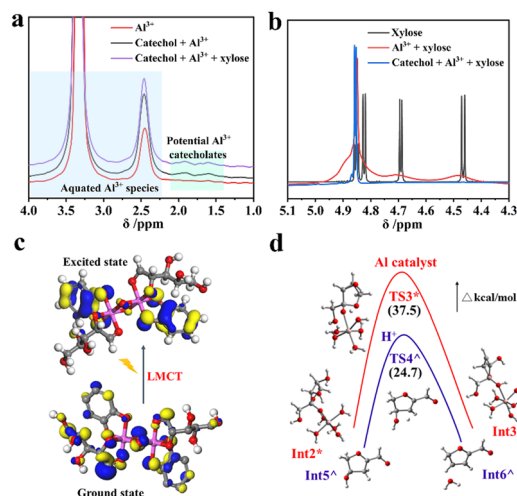


Fig. 3 (a)  $^{27}\text{Al}$  and (b)  $^1\text{H}$  NMR spectra of different reaction solutions. (c) LMCT effect of binuclear (catechol +  $\text{Al}^{3+}$  + xylose) complex. (d) Rate-determining step and energy barrier of  $\text{H}^+$  and  $\text{Al}^{3+}$  complex-catalyzed xylose dehydration.

catechol- $\text{Al}^{3+}$  complex. Compared with the sole xylose solution, the hydroxyl proton signal peaks of xylose in  $\text{Al}^{3+}$  + xylose solution were widened, and some hydroxyl proton signals of xylose in (catechol +  $\text{Al}^{3+}$  + xylose) solution were even missing, as identified by  $^1\text{H}$  NMR (Fig. 3b), which suggests the transient interaction of the catechol- $\text{Al}^{3+}$  complex with xylose at light irradiation. In contrast, the components in the reaction system are in the non-excited state under dark conditions. Meanwhile, the weak ligand (DMSO, and  $\text{H}_2\text{O}$ ) occupies the remaining  $\text{Al}^{3+}$  center after coordination with catechol, consistent with the coordination modes in Fig. S5b (ESI $^\dagger$ ).

The ground electronic states of the mononuclear metal complex (Fig. S5b, ESI $^\dagger$ ) were calculated to be mainly distributed in catechol and  $\text{Al}^{3+}$ , and the electron of the excited electronic state is transferred to the excited xylose and  $\text{Al}^{3+}$  (Fig. S7, ESI $^\dagger$ ), which are not conducive to the isomerization of xylose.<sup>13</sup> On the contrary, when the dinuclear metal complex is excited, the electron of the excited electronic state of xylose is shifted to the catechol ligand and  $\text{Al}^{3+}$ , where the LMCT effect is generated (Fig. 3c).<sup>13,14</sup> This effect can cause the transfer of electrons in xylose to the  $\text{Al}^{3+}$  coordination center, thereby reducing the electron density in the  $\beta\text{-C-H}$  bond of xylose to accelerate the isomerization process.<sup>15</sup> Meanwhile, the rate-determining energy barrier of xylulose dehydration catalyzed by Brønsted acid ( $\text{H}^+$ ) is much lower than that of the  $\text{Al}^{3+}$  complex (Fig. 3d and Fig. S8, S9, ESI $^\dagger$ ), indicating that the  $\text{H}^+$  formed by photo-induced coordination of polyphenol and  $\text{Al}^{3+}$  facilitates the dehydration.

In summary, an integrated catalytic strategy of light-enhanced acidity/local photothermal effect over a polyphenol- $\text{Al}^{3+}$  complex is presented to realize the room-temperature and quantitative synthesis of furfural from xylose under visible light irradiation.

The  $\text{Al}^{3+}$  complex has a significant absorption of light, which is conducive to the electron transfer of xylose to the coordinated  $\text{Al}^{3+}$  center (LMCT effect), thus promoting the xylose-to-xylulose isomerization. Whereafter, the light-induced coordination of  $\text{Al}^{3+}$  with polyphenols in FA facilitates the release of Brønsted acid, which is beneficial to the subsequent dehydration of xylulose. In addition, the co-added bio-graphene can not only further reinforce the acid release and LMCT effect but also produce the interfacial local photothermal effect, effectively avoiding side reactions caused by high-temperature heating of bulk solution.

The authors appreciate the National Natural Science Foundation of China (22368014, 22478087).

## Data availability

The data supporting this article have been included as part of the ESI $^\dagger$ .

## Conflicts of interest

The authors have no conflicts to declare.

## Notes and references

- 1 K. Kohse-Höinghaus, *Chem. Rev.*, 2023, **123**, 5139–5219.
- 2 (a) V. Choudhary, S. I. Sandler and D. G. Vlachos, *ACS Catal.*, 2012, **2**, 2022–2028; (b) W. Wang, J. Ren, H. Li, A. Deng and R. Sun, *Bioresour. Technol.*, 2015, **183**, 188–194.
- 3 B. Qiu, J. Shi, W. Hu, Y. Wang, D. Zhang and H. Chu, *Energy*, 2024, **294**, 130774.
- 4 Y. He, R. Zhang, W. Song, H. Liu, J. Zhang, W. Jia and L. Peng, *Chem. Eng. J.*, 2024, **480**, 148092.
- 5 W. Guo, H. C. Bruining, H. J. Heeres and J. Yue, *Green Chem.*, 2023, **25**, 5878–5898.
- 6 E. Lam, J. H. Chong, E. Majid, Y. Liu, S. Hrapovic, A. C. Leung and J. H. Luong, *Carbon*, 2012, **50**, 1033–1043.
- 7 I. Sádaba, M. Ojeda, R. Mariscal and M. L. Granados, *Appl. Catal., B.*, 2014, **150**, 421–431.
- 8 R. K. Mishra, V. B. Kumar, A. Victor, I. N. Pulidindi and A. Gedanken, *Ultrason. Sonochem.*, 2019, **56**, 55–62.
- 9 C. B. T. L. Lee and T. Y. Wu, *Renewable Sustainable Energy Rev.*, 2021, **137**, 110172.
- 10 Y. Kim, A. Mittal, D. J. Robichaud, H. M. Pilath, S. T. B. D. Etz, P. C. John, D. K. Johnson and S. Kim, *ACS Catal.*, 2020, **10**, 14707–14721.
- 11 J. Schellekens, P. Buurman, K. Kalbitz, A. V. Zomeren, P. Vidal-Torrado, C. Cerli and R. N. Comans, *Environ. Sci. Technol.*, 2017, **51**, 1330–1339.
- 12 (a) W. Wang, H. Li, J. Ren, R. Sun, J. Zheng, G. Sun and S. Liu, *Chin. J. Catal.*, 2014, **35**, 741–747; (b) I. Agirrezabal-Telleria, J. Requies, M. B. Güemez and P. L. Arias, *Appl. Catal., B.*, 2012, **115**, 169–178; (c) S. Jiang, C. Verrier, M. Ahmar, J. Lai, C. Ma, E. Muller, Y. Queneau, M. Pera-Titus, F. Jérôme and K. D. Vigier, *Green Chem.*, 2018, **20**, 5104–5110; (d) N. K. Gupta, A. Fukuoka and K. Nakajima, *ACS Catal.*, 2017, **7**, 2430–2436.
- 13 T. Tana, P. Han, A. J. Brock, X. Mao, S. Sarina, E. R. Waclawik, A. Du, S. E. Bottle and H. Y. Zhu, *Nat. Commun.*, 2023, **14**, 4609.
- 14 Y. Shi, G. Zhang, C. Xiang, C. Liu, J. Hu, J. Wang, R. Ge, H. Ma, Y. Niu and Y. Xu, *Adv. Mater.*, 2024, **36**, 2305162.
- 15 P. Han, T. Tana, S. Sarina, E. R. Waclawik, C. Chen, J. Jia, K. Li, Y. Fang, Y. Huang, W. Doherty and S. E. Bottle, *Appl. Catal., B.*, 2021, **296**, 120340.